# On the Convergence of Parallel Tempering Monte Carlo Simulations of $LJ_{38}$

**Hanbin Liu and Kenneth D. Jordan***

*Department of Chemistry and Center for Molecular and Materials Simulations, University of Pittsburgh, Pittsburgh, Pennsylvania 15260*

*Received: January 20, 2005; In Final Form: March 26, 2005*

The convergence of parallel tempering Monte Carlo simulations of the 38-atom Lennard-Jones cluster starting from the $O_h$ global minimum and from the $C_{5v}$ second-lowest-energy minimum is investigated. It is found that achieving convergence is appreciably more difficult, particularly at temperatures in the vicinity of the $O_h \rightarrow C_{5v}$ transformation when starting from the $C_{5v}$ structure. A strategy combining the Tsallis generalized ensemble and the parallel tempering algorithm is implemented and used to improve the convergence of the simulations in the vicinity of the $O_h \rightarrow C_{5v}$ transformation.

## I. Introduction

The 38-atom Lennard Jones ($LJ_{38}$) cluster has a global minimum with an $O_h$ symmetry FCC-like structure followed by a $C_{5v}$ symmetry icosahedral isomer lying only slightly higher in energy.[1,2] These two minima are separated by a complicated rearrangement pathway with a high overall barrier.[1] The funnel leading to the $C_{5v}$ potential energy minimum is much broader than that leading to the FCC minimum,[1] and as a result, it is difficult to locate the global minimum starting from an arbitrary structure and to achieve equilibrium in low-temperature Monte Carlo simulations. For these reasons, the $LJ_{38}$ cluster has proven to be a valuable system for testing global optimization and Monte Carlo simulation algorithms.[2−5]

The $LJ_{38}$ cluster, with parameters appropriate for Ar and referred to here as $Ar_{38}$, has been employed by Neirotti et al.,[3] Calvo et al.,[4] and Frantz[6] to demonstrate the utility of the parallel tempering Monte Carlo (PTMC) procedure[3,7−10] for achieving equilibrium in systems prone to quasiergodic behavior. The heat capacity curve of $Ar_{38}$ as treated classically has a pronounced peak near $T = 20$ K due to cluster melting and a weak shoulder near $T = 12$ K due to the FCC → icosahedral transition. Traditional Monte Carlo simulations with Metropolis sampling[11] are unable to characterize the $Ar_{38}$ cluster properly at temperatures in the vicinity of the latter transition. Neirotti et al. were able to overcome this problem by use the PTMC procedure in which Monte Carlo simulations are carried out for a range of temperatures and exchanges of configurations between different temperature simulations (replicas) are permitted. The PTMC simulations of Neirotti et al. employed 32 temperatures (from 0.5 to 30 K), an equilibration period of $2.85 \times 10^8$ moves, and production cycles of $1.3 \times 10^{10}$ moves at each temperature. Most moves for each replica were carried out using the Metropolis algorithm. An exchange of configurations between replicas at adjacent temperatures was attempted every 380 moves. PTMC simulations starting from the global minimum and from a randomly generated structure were found to give similar heat capacity ($C_v$) versus $T$ curves.

In testing a generalized ensemble PTMC algorithm, described below, we found that the equilibration of $Ar_{38}$ is much harder to achieve when starting the simulation from the $C_{5v}$ minimum than from the global minimum. This led us to reexamine the convergence of traditional PTMC simulations of $Ar_{38}$ starting from both the FCC global minimum and the $C_{5v}$ local minimum. In addition, we present results obtained using a parallel tempering Monte Carlo algorithm based on Tsallis statistics[12−14] (PTTS).

## II. Methodology

**A. PTMC Simulations.** The PTMC simulations carried out in the present study used the same 32 temperatures employed by Neirotti et al. Every 38th move an exchange of configurations from replicas at adjacent temperatures ($T_i$ and $T_{i+1}$) was attempted, with $T_i$ also being selected at random. This gave an attempted exchange rate of once every $38 \times 31$ moves, which is approximately three times less frequent than that used in the study of Neirotti et al. The remaining moves involved attempted displacements of individual atoms, selected at random and with acceptance/rejection being based on the Metropolis procedure. In carrying out PTMC simulations on cluster systems, it is essential to exclude evaporative events. This was accomplished in the present study by using a constraint sphere with a radius of 8.5 Å. The maximum step sizes for the production runs were determined from preliminary PTMC simulations in which the maximum step sizes were adjusted so that about 50% of the moves were accepted in each replica.

To monitor convergence, the simulations were carried out for different length equilibration periods, followed by production runs composed of $10^9$ move blocks. The equilibration periods ranged from $0.4 \times 10^9$ to $6.4 \times 10^9$ moves. The heat capacity for each simulation was calculated using

$$C_v = \frac{1}{kT^2}(\langle E^2\rangle - \langle E\rangle^2)$$

For each replica, every millionth configuration was saved for subsequent analysis.

**B. PTTS Simulations.** In the Tsallis generalized ensemble,[12−14] the entropy is defined as

$$S_q = kB\frac{\int \mathrm{d}r^N[1 - p_{\mathrm{Tsallis}}(r^N)^{q-1}]\, p_{\mathrm{Tsallis}}(r^N)}{q-1}$$

* To whom correspondence should be addressed. E-mail: jordan@pitt.edu.

10.1021/jp050367w CCC: $30.25 
Published on Web 05/20/2005

with the constraints

$$\int \mathrm{d}r^N p_{\mathrm{Tsallis}}(r^N) = 1 \qquad \text{and}$$

$$\int \mathrm{d}r^N [1 - p_{\mathrm{Tsallis}}(r^N)]^q E(r^N) = \text{constant}$$

where $q$ is a parameter greater than 1.

The generalized probability is defined as

$$p_{\mathrm{Tsallis}}(r^N) = \frac{1}{Z_q}[1 - (1-q)\beta E(r^N)]^{1/(1-q)}$$

where

$$Z_q = \int \mathrm{d}r^N [1 - (1-q)\beta E(r^N)]^{1/(1-q)}$$

When $q \rightarrow 1$, the Tsallis distribution becomes the Boltzman distribution.

The PTTS procedure carries out parallel tempering simulations with Tsallis weight functions. The implementation of the algorithm is similar to that of PTMC. The configurations are sampled with the distribution $[p_{\mathrm{Tsallis}}(r^N)]^q$ using the effective energy

$$E_{\mathrm{eff}} = \frac{q}{\beta(q-1)} \ln[1 - (1-q)\beta(E - E_0)]$$

where $E_0$ is chosen so as to lie below the energy of the global minimum.

Hansmann et al.[15] recommended choosing $q = 1 + 1/N$, where $N$ is the number of degrees of freedom in the system of interest. In the case of $Ar_{38}$, this would give $q = 1.009$. However, we were unable to achieve well-converged results for our PTTS simulations of $Ar_{38}$ with a $q$ value this large, and we adopted instead $q = 1.001$.

The probability of the acceptance of moves within individual replicas in the PTTS algorithm is given by the usual Metropolis criterion

$$P_{i \rightarrow j} = \min(1, \mathrm{e}^{-\beta(E_{\mathrm{eff},j} - E_{\mathrm{eff},i})})$$

and that for exchanges of configurations between replicas $m$ and $n$ is given by

$$P_{i \leftrightarrow j} = \min(1, \mathrm{e}^{-\Delta})$$

where

$$\Delta = \beta_m(E^m_{\mathrm{eff},j} - E^m_{\mathrm{eff},i}) - \beta_n(E^n_{\mathrm{eff},j} - E^n_{\mathrm{eff},i})$$

In our application of the PTTS algorithm, we used the same temperature grid as employed for the PTMC simulations. Evaporative events were again excluded by using a 8.5 Å constraint sphere. After the completion of the simulation, the energies were reweighted by using the histogram method[16] to transform back to the canonical ensemble.

## III. Results

**A. PTMC Simulations.** Parts a and b of Figure 1 report the heat capacity curves obtained from the PTMC simulations initiated from the $O_h$ and $C_{5v}$ minima, respectively. The various curves were obtained from simulations with production periods of $1 \times 10^9$ moves and with equilibration periods ranging from $0.4 \times 10^9$ to $6.4 \times 10^9$ moves. The curves from the simulations starting from the global minimum (Figure 1) are in fairly good agreement with one another, with the greatest sensitivity to the length of the equilibration period being for temperatures near 12 K (i.e., in the vicinity of the $O_h \rightarrow$ icosahedral transformation). The agreement in this case is even better if we consider only the simulations with equilibration periods of $3.4 \times 10^9$ or more moves. The remaining small spread in the heat capacity curves near $T = 12$ K reflects the need to use longer production runs.

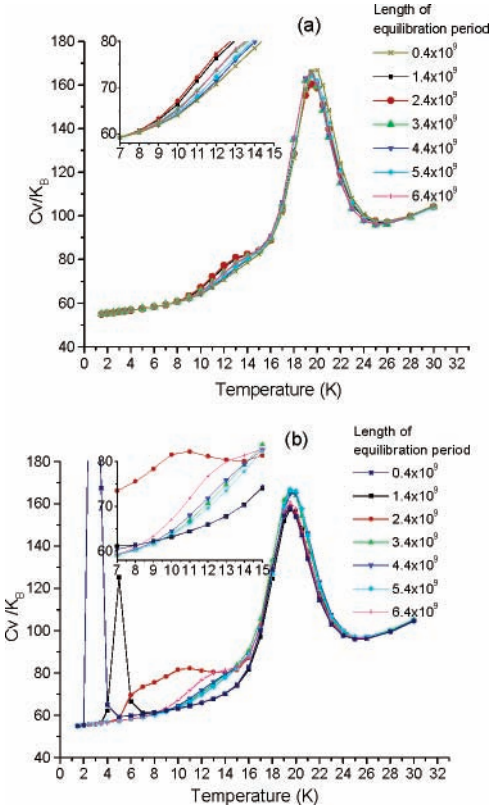


**Figure 1.** Heat capacity vs $T$ of $Ar_{38}$ from PTMC simulations (a) starting from the global minimum isomer and (b) starting from second-lowest-energy minimum isomer. All production runs were carried out for 1 billion moves. Equilibrium periods ranged from $0.4 \times 10^9$ to $6.4 \times 10^9$ moves.

From a comparison of Figure 1a and b, it is seen that the agreement between the heat capacity curves from the various simulations starting from the $C_{5v}$ minimum are much poorer than found between the heat capacity curves from the various simulations starting from the $O_h$ minimum. In particular, when starting from the $C_{5v}$ minimum, the simulations employing equilibration periods of $0.4 \times 10^9$, $1.4 \times 10^9$, and $2.4 \times 10^9$ moves display a spurious peak at temperatures below that anticipated for the $O_h \rightarrow$ icosahedral transformation. This peak is especially pronounced in the simulation with an equilibration period of only $0.4 \times 10^9$ moves, where it appears near 3 K. The spurious peak moves up in temperature and decreases in height as the equilibration period is increased, approaching the physically meaningful shoulder near $T = 12$ K for equilibration periods of $3.4 \times 10^9$ or more moves. However, even when using these longer equilibration periods, the heat capacity curves from the various simulations show more scatter, especially in the region of the $O_h \rightarrow$ icosahedral transformation when starting from the $C_{5v}$ rather than from the $O_h$ minimum. This indicates that the need for a longer production period is more acute when starting the simulation from the $C_{5v}$ minimum.

Figure 2 displays heat capacity curves obtained from PTMC simulations starting from the global minimum and from the $C_{5v}$ minimum, with equilibration periods of $3.4 \times 10^9$ moves and averaging over four consecutive blocks of $1 \times 10^9$ production

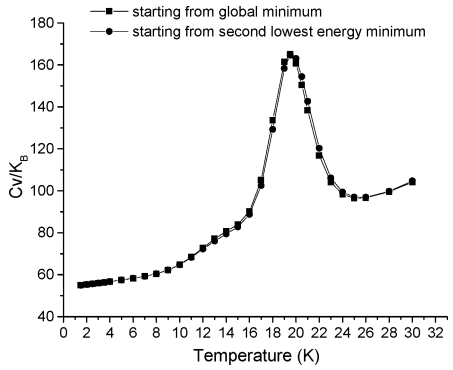


**Figure 2.** Heat capacity vs $T$ of $Ar_{38}$ from PTMC simulations starting from the global minimum and from the second-lowest-energy isomer. The equilibrium periods were $3.4 \times 10^9$ moves, and the production runs were carried out for $4 \times 10^9$ moves.

moves. The two heat capacity curves are in close agreement with one another as well as with that published previously by Neirotti et al. even in the region of the shoulder due to the $O_h \rightarrow$ icosahedral transformation. However, the agreement is deceptive as is revealed by comparing with the results obtained from still longer simulations with averages calculated using the configurations sampled in the moves between $7.4 \times 10^9$ and $11.4 \times 10^9$ and between $11.4 \times 10^9$ and $17.4 \times 10^9$. For the case in which the simulations were started from the global minimum, the resulting heat capacity curves are nearly identical to that obtained by averaging over the configurations sampled over $3.4 \times 10^9$ to $7.4 \times 10^9$ moves, as shown in Figure 2. However, in the case in which the simulations were started from the second-lowest-energy minimum, the heat capacity curve obtained by averaging over configurations sampled in the $7.4 \times 10^9$ to $11.4 \times 10^9$ range of moves is much more pronounced than that reported in Figure 2, whereas that obtained by averaging over moves in the $11.4 \times 10^9$ to $17.4 \times 10^9$ range is similar to that reported in Figure 2. These results show that very long production runs are required to achieve convergence of PTMC simulations in the vicinity of the $O_h \rightarrow$ icosahedral transformation when starting from the $C_{5v}$ minimum.

Additional insight into the origin of the difficulty in converging the PTMC simulations of $LJ_{38}$ when starting from the $C_{5v}$ minimum can be gained by determining the inherent structures associated with the configurations present at the end of each equilibration period. The inherent structures were obtained by optimizing the structures with the eigenmode-following algorithm[17,18] as implemented in the Orient program.[19] Figure 3a reports for the simulations starting from the global minimum the energies of the resulting inherent structure at the end of various equilibration periods. The resulting inherent structure distributions are similar for various-length equilibration periods, with the first 10 replicas (i.e., those for the 10 lowest temperatures) giving the global minimum and at most 3 of the 17-lowest-temperature replicas giving an inherent structure other than the global minimum. Similar results are found for the inherent structures populated at the end of the production runs for the simulations starting from the $C_{5v}$ local minimum for the cases of equilibration periods of $3.4 \times 10^9$ or more moves (Figure 3b). However, in the simulations with equilibration periods of $2.4 \times 10^9$ or fewer moves, fewer low-temperature replicas have inherent structure associated with the global minimum at the end of the equilibration runs. In fact, with an equilibration period of only $0.4 \times 10^9$ moves only the lowest-temperature replica is associated with the global minimum inherent structure at the end of the equilibration. As the production runs increase from $4 \times 10^8$ to $3.4 \times 10^9$ moves, the

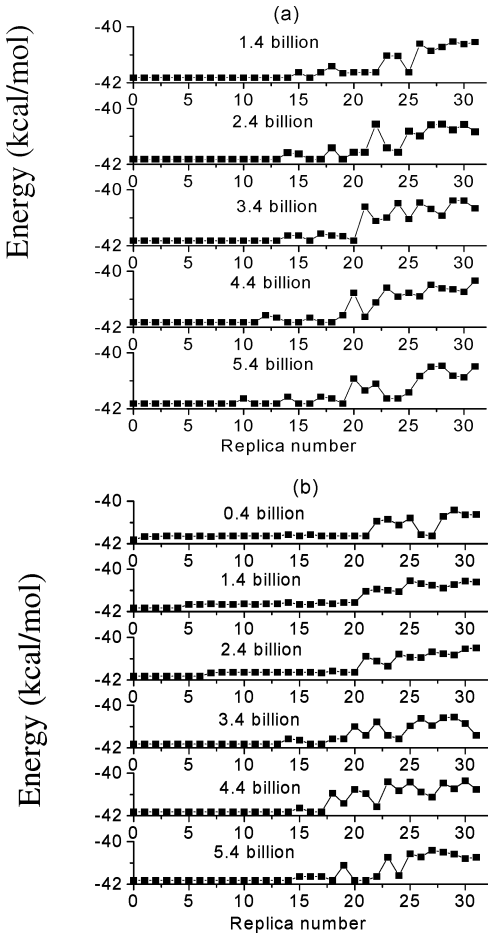


**Figure 3.** Inherent structures at the end of various-length equilibration periods for PTMC simulations of $Ar_{38}$ (a) starting from the global minimum and (b) starting from the second-lowest-energy minimum. The number of moves in each equilibration period is specified.

number of low-temperature replicas associated with the global minimum at the end of the run increases. The spurious low-temperature peak in the heat capacity curve in the simulations starting from the second-lowest-energy minimum structure and with equilibration periods of less than $3.4 \times 10^9$ moves is a consequence of the global minimum structure not being adequately sampled in the equilibration runs in the low-temperatures replicas. In these cases, during the course of the production runs, there is a shift in the population in the low-temperature replicas from minima in the icosahedral funnel to the $O_h$ funnel. This shift in population is responsible for the spurious low-temperature peak in $C_v$. Although this problem could be overcome by the use of very long production cycles, this is less computationally efficient than using equilibration runs of adequate length.

We next examine the distributions of inherent structures obtained from the production runs associated with PTMC simulations starting from both the global minimum structure as well as from the $C_{5v}$ minimum. Figure 4 shows the distributions obtained for the simulations starting from the $C_{5v}$ local minima using production runs of $1 \times 10^9$ moves and employing various-length equilibration periods. For each simulation, every millionth configuration was saved and optimized to its inherent structure. It is clear from the results reported in this Figure that the simulations using equilibration periods of only $1.4 \times 10^9$ and $2.4 \times 10^9$ moves are far from converged.

Figure 5 reports the distributions of inherent structures from simulation starting from the $O_h$ and $C_{5v}$ minima and carried out

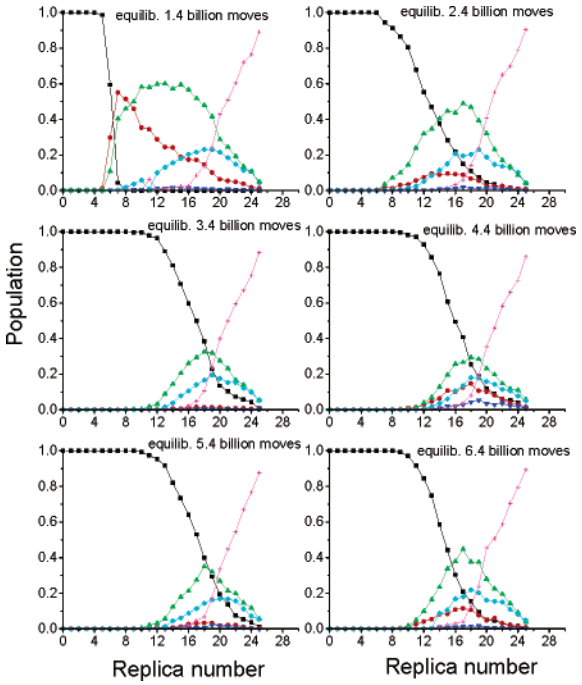


**Figure 4.** Inherent structure distributions from PTMC simulations of $Ar_{38}$ starting from the second-lowest-energy minimum. The simulations were carried out with a production period of $1 \times 10^9$ moves and differ in the length of the equilibrium period. The inherent structures are labeled as follows: ■, $E = -41.821$; ●, −41.659; ▲, −41.630; ▼, −41.588; ◆, −41.569; and +, >−41.569 kcal/mol. The inherent structures with energies of −41.821 and −41.659 kcal/mol are the global minimum and the second-lowest-energy minimum, respectively.

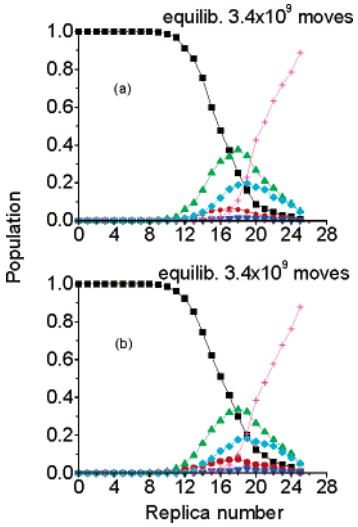


**Figure 5.** Inherent structure distributions from PTMC simulations of $Ar_{38}$ starting from (a) the global minimum and (b) the second-lowest-energy minimum. The simulations were carried out with an equilibration period of $3.4 \times 10^9$ moves and production runs of $4 \times 10^9$ moves. The inherent structures are labeled as follows: ■, $E = -41.821$; ●, −41.659; ▲, −41.630; ▼, −41.588; ◆, −41.569; and +, >−41.569 kcal/mol.

for equilibration periods of $3.4 \times 10^9$ moves and production periods of $4 \times 10^9$ moves. The inherent structure distributions from these two simulations are nearly identical, although, as pointed out above, simulations starting from the second-lowest-energy minimum are not actually converged. The population of low-energy structures associated with the icosahedral funnel grows rapidly as the temperature increases from about 10 K

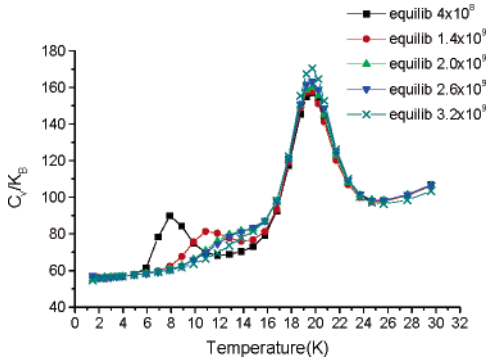


**Figure 6.** Heat capacity vs $T$ of $Ar_{38}$ from PTTS simulations starting from the second-lowest-energy minimum. Equilibration periods ranged from $0.4 \times 10^8$ to $2.6 \times 10^9$ moves, and production periods were $1 \times 10^9$ moves for the case of an equilibration period of $0.4 \times 10^8$ moves and $0.6 \times 10^9$ moves in the other four cases.

and reaches a maximum around 18 K. Interestingly, both the third- and fifth-lowest-energy isomers of $Ar_{38}$ acquire considerably more population than does the second-lowest-energy ($C_{5v}$) isomer. At $T = 18.5$ K, 65% of the total population is associated with the four-lowest-energy inherent structures associated with the icosahedral funnel.

**B. PTTS Simulations.** Figure 6 shows the heat capacity curves obtained from the PTTS simulations of $Ar_{38}$ initiated from the second-lowest-energy minimum. The equilibration periods ranged from $0.4 \times 10^9$ to $3.2 \times 10^9$ moves and the production cycles were either $1.0 \times 10^9$ or $0.6 \times 10^9$ moves. PTTS simulations with an equilibration period as short as $2.0 \times 10^9$ moves and a production period as short as $0.6 \times 10^9$ moves give a nearly converged $C_v$ versus $T$ curve, with the exception being that the shoulder near 12 K is slightly more pronounced than found from the PTMC simulations starting from the global minimum. Upon adoption of an equilibration period of $3.2 \times 10^9$ moves, while retaining a production period of only $0.6 \times 10^9$ moves, the low-temperature shoulder is attenuated, bringing it more in line with the results from the PTMC simulations starting from the global minimum structure. The more rapid convergence of the PTTS simulations compared to that of the PTMC simulations may be a consequence of the broader potential energy distributions associated with the former.

## IV. Conclusions

The present study demonstrates that it is much more difficult to achieve equilibrium in PTMC simulations on the $Ar_{38}$ cluster when starting from the second-lowest-energy minima than when starting from the global minimum. Although not discussed in the text, we have also found that simulations starting from the third-lowest-energy minimum, which, as with the second-lowest-energy isomer, is associated with the icosahedral funnel, also require long production and equilibration periods to achieve convergence. We anticipate that this is also the case for other low-energy minima associated with the icosahedral funnel. It is known from the work of Wales and Doye[20] that when starting from an arbitrary structure it is easier to locate the $C_{5v}$ minimum than the $O_h$ minimum of $LJ_{38}$. On the basis of the results of the present study, we conclude that it is more difficult to escape from the $C_{5v}$ minimum than from the $O_h$ minimum. This is consistent with the finding of Wales,[21] who, using information on the minima and transition states of $LJ_{38}$, calculated rates for escaping from these two minima, and is a consequence of the $O_h$ minimum being associated with a narrow funnel and the $C_{5v}$ minimum being associated with a broad funnel on the

potential energy surface. Thus the $LJ_{38}$ cluster with the initial configuration chosen to be a minimum in the icosahedral funnel should serve as a valuable test case for new Monte Carlo simulation algorithms.

**Acknowledgment.** We thank Professor David Freeman for valuable discussions of the parallel tempering procedure. This research was supported by a grant from the National Science Foundation through grant number CHE-0078528.

## References and Notes

(1) Doye, J. P. K.; Miller, M. A.; Wales, D. J. *J. Chem. Phys.* **1999**, *110*, 6896.
(2) Doye, J. P. K.; Wales, D. J.; Miller, M. A. *J. Chem. Phys.* **1998**, *109*, 8143.
(3) Neirotti, J. P.; Calvo, F.; Freeman, D. L.; Doll, J. D. *J. Chem. Phys.* **2000**, *112*, 10340.
(4) Calvo, F.; Neirotti, J. P.; Freeman, D. L.; Doll, J. D. *J. Chem. Phys.* **2000**, *112*, 10350.
(5) Bayden, A. S.; Jordan, K. D. *Chem. Phys. Lett.* **2004**, *385*, 101.
(6) Frantz, D. D. *J. Chem. Phys.* **2001**, *115*, 6136.
(7) Tesi, M. C.; vanRensburg, E. J. J.; Orlandini, E.; Whittington, S. G. *J. Stat. Phys.* **1996**, *82*, 155.
(8) Marinari, E.; Parisi, G. *Europhys. Lett.* **1992**, *19*, 451.
(9) Geyer, C. J.; Thompson, E. A. *J. Am. Stat. Assoc.* **1995**, *90*, 909.
(10) Pillardy, J.; Piela, L. *J. Phys. Chem. A* **1995**, *99*, 11805.
(11) Metropolis, N.; Rosenbluth, A. W.; Rosenbluth, M. N.; Teller, A. H.; Teller, E. *J. Chem. Phys.* **1953**, *21*, 1087.
(12) Tsallis, C. *J. Stat. Phys.* **1988**, *52*, 479.
(13) Tsallis, C.; Stariolo, D. A. *Physica A* **1996**, *233*, 395.
(14) Andricioaei, I.; Straub, J. E. *Phys. Rev. E* **1996**, *53*, R3055.
(15) Hansmann, U. H. E.; Okamoto, Y. *Braz. J. Phys.* **1999**, *29*, 187.
(16) Ferrenberg, A. M.; Swendsen, R. H. *Phys. Rev. Lett.* **1988**, *61*, 2635.
(17) Cerjan, C. J.; Miller, W. H. *J. Chem. Phys.* **1981**, *75*, 2800.
(18) Wales, D. J. *Mol. Phys.* **1991**, *74*, 1.
(19) Stone, A. J.; Dullweber, A.; Engkvist, O.; Fraschini, E.; Hodges, M. P.; Meredith, A. W.; Popelier, P. L. A.; Wales, D. J. *Orient: a Program for Studying Interactions between Molecules*, version 4.5; University of Cambridge: 2003.
(20) Wales, D. J.; Doye, J. P. K. *J. Phys. Chem. A* **1997**, *101*, 5111.
(21) Wales, D. J. *Mol. Phys.* **2002**, *100*, 3285.